Proceedings of the Institute of Acoustics

Approximations for the Maximum Amplitude of Higher-Order Duct Modes

J.L. Horner Loughborough University, Dept of Aeronautical and Automotive Engineering, UK
R. Lyons Loughborough University, Dept of Civil and Building Engineering, UK
B.A.T. Petersson Loughborough University, Dept of Aeronautical and Automotive Engineering, UK

1. INTRODUCTION

There are many engineering problems which involve determining the sound fields resulting from an incident wave, of arbitrary angle, impinging on a circular orifice in a rigid wall of finite thickness. In order to obtain a full solution for the reflected, scattered, in-orifice and transmitted fields, it is necessary to determine the effect of modal coupling[1]. Previous authors[2] have used a Hankel transform approach to obtain a more rigorous solution to the problem. A matrix formulation of the problem was used to estimate the velocity potentials of the four fields and validated using experimental data. In this study, the expressions, which describe the modal energy in the scattered field have been further investigated in order to establish the contribution of higher order modes to the field[3].

The work on the effects of modal coupling has been extended here to include a method of simply approximating the complex amplitude of the forward and backward waves in the duct at the cut-on wavenumber, based only on knowledge of the modal wave number. The technique has been established by investigating the relationship between the peak values of the driving functions and modal wavenumber. Once simple approximations are established for the in-duct field, it is possible to predict the maximum amplitude of both the scattered and transmitted fields for the system. Results from the approximate method are compared to the results from a fully coupled solution for the orifice system.

2. DESCRIPTION OF ACOUSTIC FIELD

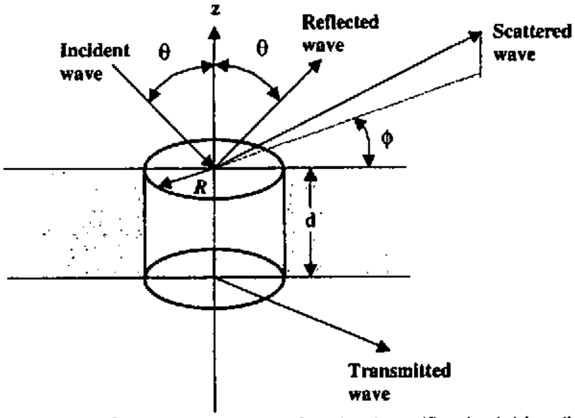

Figure 1, Co-ordinate system for circular orifice in rigid wall.

Consider a circular orifice of radius *R* in a rigid wall as indicated in Figure 1. Following Ref. 2 the velocity potential for an incident wave of arbitrary angle, *θ*, may be given by

$$\Phi^i(r,\phi,z) = e^{-ikz\cos\theta} \sum_{m=-\infty}^{\infty} i^m J_m(kr\sin\theta)\, e^{im\phi} \quad (1)$$

The resulting reflected and scattered velocity potentials are given by

$$\Phi^r(r,\phi,z) = e^{ikz\cos\theta}\sum_{m=-\infty}^{\infty} i^m J_m(kr\sin\theta)\, e^{im\phi}\,,$$

$$\Phi^s(r,\phi,z) = \sum_{m=\infty}^{\infty} e^{im\phi}\int_0^{\infty}\tilde{\Phi}^{s_m}(\zeta)\, J_m(\zeta\, r)\, e^{i\kappa z}\zeta d\zeta\,. \tag{2}$$

where the scattered wavenumber, $\kappa = \sqrt{k^2-\zeta^2}$. Inside the orifice the field is given over the depth *d*, by

$$\Phi^d(r,\phi,z) = \sum_{n=-\infty}^{\infty} e^{im\phi}\sum_{n=-\infty}^{\infty}\left[\, b_n^m \sin k_z(z+d) + c_n^m \cos k_z(z+d)\right]\, J_m(k_n r) \tag{3}$$

where the wave number in z-direction, $k_z = \sqrt{k^2-k_n^2}$. Assuming a rigid wall surrounding the orifice, the velocity potential gradients may be summed for the orifice area and regions outside. Applying a Hankel transform to the two expressions determined from the summed velocity potential gradients, yields the following expressions[2]:

$$\tilde{\Phi}^{s_m}(\zeta) = \frac{-i}{\kappa}\sum_{n=1}^{\infty} k_z\left(-c_n^m \sin k_z d + b_n^m \cos k_z d\right)\, I^m(k_n,\zeta) \tag{4}$$

in which

$$I^m(k_n,\zeta) = \begin{cases} \dfrac{R}{k_n^2-\zeta^2}\left[k_n J_{m+1}(k_n R)\, J_m(\zeta R) - \zeta J_m(k_n R)\, J_{m+1}(\zeta R)\right] & k_n \neq \zeta, \\ \dfrac{R^2}{2}\left[\, J_m^2(k_n R) - J_{m-1}(k_n R)\, J_{m+1}(k_n R)\right] & k_n = \zeta. \end{cases} \tag{5}$$

Also by equating the velocity potentials on the incident side of the orifice, it may be shown that[2],

$$\left(c_p^m \cos k_z d + b_p^m \sin k_z d\right) I^m(k_p,k_p) + \sum_{n=1}^{\infty} ik_z\left(b_n^m \cos k_z d - c_n^m \sin k_z d\right) I_{np}^m = 2i^m I^m(k\sin\theta, k_p) \tag{6}$$

where $$I_{np}^m = \int_0^{\infty}\kappa^{-1} I^m(k_n,\zeta) I^m(k_p,\zeta)\zeta d\zeta\,, \tag{7}$$

and *(m,n)* is the mode of interest and *(m,p)* is any other higher mode of the duct. Equating velocity potentials and gradients of velocity potential, respectively, on the outlet side of the orifice, gives in accordance with Ref. 2,

$$c_p^m I^m\left(k_p,k_p\right)-\sum_{n=1}^{\infty} ik_z b_n^m I_{np}^m = 0 \tag{8}$$

Thus Eqs. (6) and (8) must be solved for *p* number of modes in order to determine the coupled in-duct wave amplitudes b_n^m and c_n^m. Previous work[3] has shown that at the cut-on wavenumber ($\zeta = k_n$ and $k\sin\theta = k_n$) the contributions from other higher modes are zero due to the orthogonality of functions $I^m\left(k_n,\zeta\right)$ (Eqn 5). As $I^m\left(k_n,\zeta\right)$ is zero at all cut-on wavenumbers other than the mode of interest, then the only contribution to the amplitude of the scattered field (Eq. 4) at the wavenumber, $k_n = \zeta$, is the single (*m,n*) mode. At wavenumbers other than a cut-on wavenumber, the function $I^m\left(k_n,\zeta\right)$ is non-zero and all cut-on modes contribute to the scattered and transmitted fields. Therefore, if equations (6) and (8) are solved for a single uncoupled (*m,n*) mode, assuming $\zeta = k_n$, then b_n^m and c_n^m are given by

$$b_n^m = \frac{I^m\left(k_n,k_n\right)\gamma_n^m}{\Delta}\ ,\ c_n^m = \frac{ik_z I_{nn}^m \gamma_n^m}{\Delta} \tag{9,10}$$

where $\Delta = \left(k_z^2 {I_{nn}^m}^2 + I^m\left(k_n,k_n\right)\right)^2 \sin k_z d + 2ik_z I_{nn}^m I^m\left(k_n,k_n\right)\cos k_z d$, and

$\gamma_n^m = 2i^m I^m\left(k\sin\theta,k_n\right)$.

Thus to calculate simply b_n^m and c_n^m it is necessary to evaluate the forcing terms, I_{nn}^m, $I^m\left(k_n,k_n\right)$ and γ_n^m at the cut-on wave number of the mode of interest.

3. FORCING FUNCTIONS $I^m\left(k_n,k_n\right)$ AND $I^m\left(k\sin\theta,k_n\right)$

Using a Hankel transform approach, allows the three dimensional problem of scattering from an orifice to be reduced to a two dimensional one, were the system may be considered to be driven in the z - ϕ plane. Thus the function $I^m\left(k_n,\zeta\right)$ represents the excitation as a function of the recoil wavenumber, ζ and the function $I^m\left(k\sin\theta,k_n\right)$ represents the excitation as a function of the projected wavenumber, $k\sin\theta$. If both functions are plotted against normalised wavenumber (Figure 2), it may be seen that the functions are identical for each (*m,n*) mode. Previously an expression was determined for the peak value of the forcing function using simple curve fitting and was found to be[3]

$$I^m\left(k_n,\zeta\right) = \mathrm{a}\,R\,k_n^{-\mathrm{b}} \tag{11}$$

where: a = 0.30, b = 0.98 $n > 1$
a = 0.25, b = 1.10 $n = 1$

The modes where n =1, those with no circumferencial nodal lines, peak at a wave number greater than $\zeta = k_n$ (Figure 2) and the peak value is controlled by different constants[3].

4. FORCING FUNCTION I_{nn}^m

The forcing function, I_{np}^m is determined from the integral given in Eq. (7) and represents the contribution of a mode (*m,p*) to the 'driving field' for the scattering of the mode of interest (*m,n*). Thus when fully considering the resulting scattered field for the (*m,n*) mode, a contribution must be inculded for every other mode. When calculating a single mode contribution, I_{nn}^m, the mode of interest (*m,n*) only is considered.

Figure 3 shows the real part of I_{np}^m plotted against *n* for the *m* =1 set of modes, *n* =1 to 10. Other values of *m* were investigated and the following observations hold for all *m* values. For the set of data shown, the radius *R* = 1.0m and the duct length *d* = 0.1m. This particular aspect ratio of duct was chosen to allow a significant number of modes to propagate in the duct. In Figure 3, shown as logarithmic data to indicate differences, the curve represents the values of I_{nn}^m, the real part of the forcing function with only a single mode contributing to the field. The other data points represent the ninety values of I_{np}^m, the real part of the forcing function for a mode (*m,n*) with a contribution from another mode (*m,p*). It can be observed that the I_{nn}^m data set is some three orders of magnitude greater than the I_{np}^m data set. Also it can be observed that the I_{nn}^m data set forms a curve reducing in magnitude as *n* increases. From examining the values of the real part of I_{nn}^m for other aspect ratios and mode numbers, it is found that for each *m* set, curves could be plotted through the real part of I_{nn}^m. By applying simple curve fitting techniques to various sets of data for the real part of I_{nn}^m, it is possible to establish the following empirical relationships. It should be noted that there are three different governing relationships depending on the mode number.

For $m = 0$, $n > 1$ set of modes:

$$\mathrm{Re}\left(I_{nn}^0\right) = 4.00 \times 10^{-3}\ R^2\ n^{-1.30} \tag{12a}$$

For $m \neq 0$, $n = 1$ set of modes:

$$\mathrm{Re}\left(I_{11}^m\right) = 4.86 \times 10^{-3}\ R^2\ \left(k_r R\right)^{-1.12} \tag{12b}$$

For $m \neq 0$, $n \neq 1$ set of modes:

$$\mathrm{Re}\left(I_{nn}^m\right) = 2.54 \times 10^{-3}\ R^2\ m^{-0.70} n^{\alpha}, \text{ where } \alpha = -1.08\, m^{-0.39} \tag{12c}$$

Table 1 shows the relative error between the real part of I_{nn}^m calculated using Eqs. (5) and (7) and the real part calculated using Eqs. (12a - 12c). For this example *R* = 0.6m and *d* = 0.2m, to ensure cut-on of higher modes. Note that it is not possible to determine the real part of I_{nn}^m for the (0,1) mode using Eq. (12) as k_n = 0. As the amplitude of this mode is simple to predict, it is no disadvantage to the proposed method. Also it may be observed that the relative error increases with increasing modal wavenumber. Application of a more complex curve fitting routine may result in reducing this error at high modal wavenumbers.

Mode	Error in Real Part of I^m_{nn} (%)
0,2	0.4
0,3	-3.8
0,4	0.03
0,5	6.7
2,1	3.4
2,2	3.6
2,3	4.0
2,4	5.7
2,5	9.5

Table 1: Relative error in Real Part of I^m_{nn}

Examining the imaginary parts of I^m_{np}, shows that it is always two orders of magnitude smaller than the real part of the function, for a free field situation. As the real part of the forcing function I^m_{nn} dominates, it is assumed that only the real part needs to be evaluated for an approximate solution. Also, it is assumed that the real part of I^m_{np} represents the propagating part of the scattered field. In the following section, the error introduced by this approximation will be examined.

5. PREDICTION OF MAXIMUM IN-DUCT WAVE AMPLITUDES

Eqs. (9) and (10) are expressions for the amplitudes of the in-duct waves uncoupled from any other mode. In previous investigations[3], it was found that at the cut-on wave number of the mode, only the mode of interest contributes to the in-duct amplitude. The function $I^m(k_n,\zeta)$, Eq. (5), is a maximum at $\zeta = k_n$ and is zero at $\zeta = k_p$. Thus in the expression for the amplitude of the scattered field, Eq. (4), only the (*m*,*n*) mode will be non-zero at $\zeta = k_n$. Thus at recoil wavenumbers other than those equal to modal wavenumbers, all modes contribute to the system response. At recoil wavenumbers that equal modal wavenumbers, only a single mode contributes to the total response. As cut-on for a mode occurs when there is coincidence between the driving wave number and the recoil and modal wavenumbers, then the three forcing functions will be a maximum. Thus it is possible to predict the maximum of the three forcing functions using Eqs. (11) and (12). Once the three maximum forcing functions are known, it is possible to substitute the values into Eqns. (9) and (10) to predict the approximate maximum in-duct amplitudes.

Tables 2 and 3 show the comparison between the approximate and fully coupled solutions of the in-duct wave amplitudes at cut-on for the mode of interest. Approximate values were determined using Eqns. (9) - (12) and are shown as a ratio of the response at cut-on from a fully coupled solution using Eqns. (5) - (8). For this comparison the radius R = 0.6m and the depth d = 0.2m. The fully coupled solution used ten modes to calculate the modal sum. From observation the fully coupled calculation appeared stable after five modes were added to the sum. The driving wavenumber was set to $k = 50\text{m}^{-1}$

for all modes. Each table provides the ratio of both the real and imaginary parts and the modulus and phase of the wave amplitudes. Thus a unity value represents full agreement between the approximate and full solutions.

	$b_n^m\left(\frac{Approximate}{Fullycoupled}\right)$				$c_n^m\left(\frac{Approximate}{Fullycoupled}\right)$			
Mode	Modulus	Phase	Real	Imaginary	Modulus	Phase	Real	Imaginary
0,2	1.02	0.99	0.98	1.03	1.01	1.00	1.00	1.01
0,3	0.97	0.99	0.89	0.98	1.00	1.00	1.00	1.01
0,4	1.05	0.98	-1.14	1.05	1.04	1.00	1.04	1.04
0,5	1.11	0.98	1.17	1.10	1.03	1.00	1.03	1.04

Table 2: Ratio of approximate - fully coupled solutions for modes (0,2) - (0,5) (Rounded to 2dp)

Table 2 is for the set of modes (0,2-5). The mode (0,4) appears to have an error of -14% in the real part of b_n^m. This particular mode, for this example, had a maximum real part of almost zero, and the approximate solution resulted in a small negative number rather than a small positive number. The imaginary part of the same wave has a difference of 10% or less. When comparing the modulus and phase for the two solutions of b_n^m mode (0,4), it may be observed that the error is acceptable, being 5% for the modulus and 2% for the phase. The opposing wave, c_n^m, may be observed to yield smaller differences than the b_n^m wave for all four modes.

	$b_n^m\left(\frac{Approximate}{Fullycoupled}\right)$				$c_n^m\left(\frac{Approximate}{Fullycoupled}\right)$			
Mode	Modulus	Phase	Real	Imaginary	Modulus	Phase	Real	Imaginary
2,1	0.98	1.04	0.92	1.00	0.93	0.92	0.93	1.00
2,2	1.13	1.02	1.04	1.14	1.03	1.03	1.03	1.01
2,3	1.10	1.02	0.21	1.10	1.04	1.04	1.02	1.00
2,4	1.09	1.02	1.18	1.07	1.01	1.01	1.02	1.00
2,5	1.13	1.02	1.16	1.06	1.01	1.00	1.01	1.00

Table 3: Ratio of approximate - fully coupled solutions for modes (2,1) - (2,5) (Rounded to 2dp)

For Table 3, the *m* number is increased, to show the results for the modes (2,1-5). Apart from the real part of b_n^m of mode (2,3), the error is again within acceptable bands. For the b_n^m wave for mode (2,3), the difference appears to be some 80% of the fully coupled calculation. On inspection of the data for this mode, it was found that the real part of b_n^m, determined from the full calculation, was about an order of magnitude smaller than the real parts of other modes, with the wave amplitude being almost wholly imaginary. The approximate method also yielded a small real part for this wave, but some 80% in error. The imaginary part of b_n^m (2,3) mode has an acceptable 10% error, leading to the modulus of the wave amplitude of the (2,3) mode to have an error of 10%. For both the real and imaginary parts of the c_n^m wave the error is small with the (2,1) mode having an error of approximately 7% and the other four modes having an error of less than 3%.

The two data sets were selected to show cases where apparently large errors in the real part of the solution from the approximate calculations lead to acceptable errors in both the modulus and phase of the amplitudes. It can be observed from the data sets, that the errors in the calculation of c_n^m are always smaller than the errors in the calculation of b_n^m.

6. DISCUSSION

In previous investigations it has been established that at the cut-on wave number for a higher mode in a duct only the mode of interest contributes to the field at that wave number. By following a Hankel transform solution for the fields resulting from the impingement of a wave on a circular orifice in a hard wall, it is possible to obtain an expression for the uncoupled higher mode wave amplitudes in the duct. These wave amplitudes depend on the dimensions of the duct, the modal and axial wave numbers and three forcing functions. The forcing functions can be considered to consist of a driving term in the radial plane, a driving term in the axial plane and a term describing the coupled driving field for the scattered field. By investigating each of the driving terms individually it was found that simple approximate expressions could be obtained for the peak load, at cut-on, for each (m,n) mode. For the radial and axial driving terms, the approximate expression was a function of duct radius and modal wave number. Although the modal wave number may be considered to only drive the radial field, the axial and radial forcing functions are identical at cut-on and hence both may be described using the same expression. The approximate expression for the driving term, dependent on the scattered field, is a function of both (m,n), duct radius and the modal wave number.

When the maximum values for the three driving terms are substituted into the expressions for the uncoupled in-duct wave amplitudes it is possible to obtain an approximate complex amplitude for a particular cut-on mode. As the amplitude of any mode will be greatest at cut-on, the approximate value represents the maximum possible amplitude. Comparison of the approximate solutions with the solutions from a fully coupled calculation shows good agreement. The maximum error occurrs in the forward wave.

The advantage of the method presented above is that it allows easy calculation of the maximum possible in-duct modal wave amplitudes for a system. By obtaining maximum values for each mode, it is possible, for a particular driving wavenumber, to establish the dominant contribution. It should be noted that the method only works for modes that are cut-on in the duct. If the duct mode is not cut on, it would not be possible to generate a reflected wave in the duct and the in-duct expressions would be in error.

7. REFERENCES

1. Morse, P.M. and Ingard, K.V. 'Theoretical Acoustics', New Jersey, Princeton Press, 1986, Ch 9.
2. Jun, K.T.L and Eom, H.J. 'Acoustic Scattering from a circular aperture in a thick hard screen' J Acoust. Soc. Am. 98(4) pp 2324-2327 (1995)

3. Horner, J. L, Lyons, R. and Petersson, B.A.T. 'Approximations for modal coupling in scattered fields from orifices' submitted to J.Acoust. Soc.Am (Jan 2000)

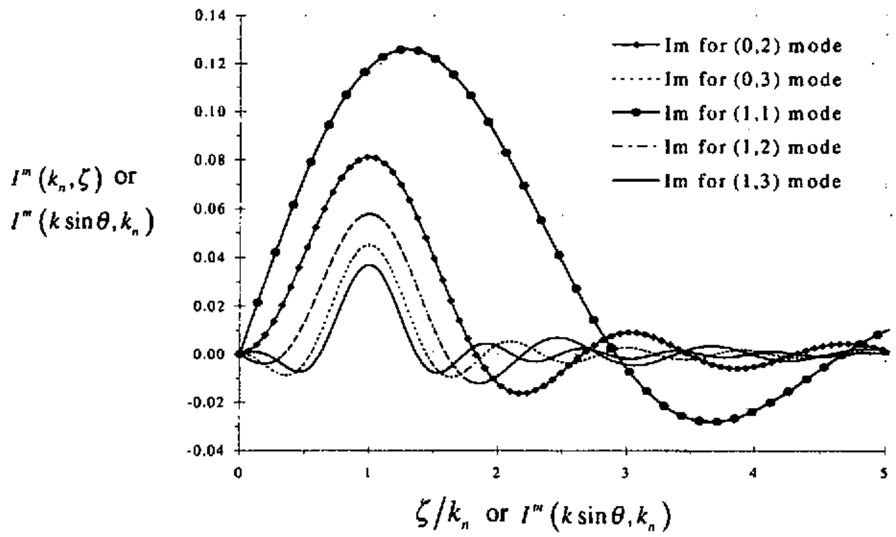

Figure 2. $I^m(k_n,\zeta)$ and $I^m(k\sin\theta,k_n)$ for various modes.

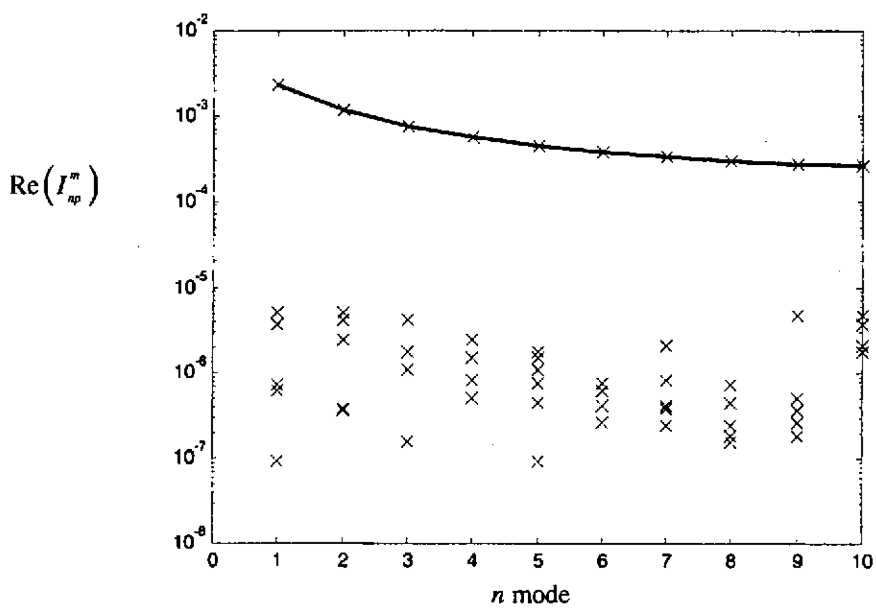

Figure 3. Real part of the Forcing Function